

2

FTD-ID(RS)T-0106-89

AD-A208 901

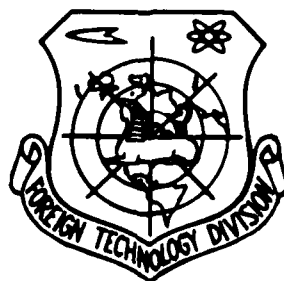
FOREIGN TECHNOLOGY DIVISION



A POSITRON CT CAMERA SYSTEM USING MULTIWIRE PROPORTIONAL CHAMBERS
AS DETECTORS

by

Wang Dewu, Shen Guilin, et al.



DTIC
ELECTE
JUN 13 1989
S E D

Approved for public release;
Distribution unlimited.



053

HUMAN TRANSLATION

FTD-ID(RS)T-0106-89 18 May 1989

MICROFICHE NR: FTD-89-C-000355

A POSITRON CT CAMERA SYSTEM USING MULTIWIRED
PROPORTIONAL CHAMBERS AS DETECTORS

By: Wang Dewu, Shen Guilin, et al.

English pages: 14

Source: Gaoneng Wuli Yu He Wuli, Vol. 12,
Nr. 3, May 1988, pp. 289-297

Country of origin: China

Translated by: Leo Kanner Associates
F33657-88-D-2188

Requester: FTD/SDMS/Lt Paul Lithgow
Approved for public release; Distribution unlimited.

THIS TRANSLATION IS A RENDITION OF THE ORIGINAL FOREIGN TEXT WITHOUT ANY ANALYTICAL OR EDITORIAL COMMENT. STATEMENTS OR THEORIES ADVOCATED OR IMPLIED ARE THOSE OF THE SOURCE AND DO NOT NECESSARILY REFLECT THE POSITION OR OPINION OF THE FOREIGN TECHNOLOGY DIVISION

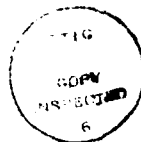
PREPARED BY:

TRANSLATION DIVISION
FOREIGN TECHNOLOGY DIVISION
WPAFB, OHIO

GRAPHICS DISCLAIMER

All figures, graphics, tables, equations, etc. merged into this translation were extracted from the best quality copy available.

Accession For	
NTIS GRA&I	<input checked="" type="checkbox"/>
DTIC TAB	<input type="checkbox"/>
Unannounced	<input type="checkbox"/>
Justification	
By	
Distribution/	
Availability Codes	
Dist	Avail and/or Special
A-1	



A POSITRON CT CAMERA SYSTEM USING MULTIWIRE
PROPORTIONAL CHAMBERS AS DETECTORS

Wang Dewu, Shen Guilin, Na Shuzhen, Li Yunshan, Li Chengze, Li Zhigang,
Chen Kun, Chen Yuanbo, Chen Zhiping, Ma Mei, Shen Miaohe,
Zhao Haiquan, Lou Jiashu, Xu Rongfen

(Institute of High Energy Physics, Academia Sinica, Beijing)

Abstract

This article reports on a positron computerized tomography camera system using multiwire proportional chambers (MWPC) as detectors. This system is composed of two high-density MWPC gamma-ray detectors, an electronic readout system and a computer for data processing. Three-dimensional tomography is obtained. The imaging matrix is $64 \times 64 \times 16$.

1. Introduction

The appearance of x-ray computerized tomography (XCT) is a great pioneering work in the field of medical imaging, encouraging those involved in nuclear medicine to bring to fulfillment their aspirations for three-dimensional radiography. Nuclides emitting positrons are used as the tracer; electrons from within the human body and these positrons are annihilated, and a pair of gamma rays is emitted in opposite directions. Use of the appropriate technique to measure these two rays makes it possible to obtain information on direction and position. Tomographs produced by positrons (called PECT) are one of the best means available to the medical imaging field for realizing three-dimensional description; what they provide is not merely anatomical information; their more important value lies in the transmission of information on normal and abnormal human chemistry and physiology [1]. In nuclear medicine, the use of PECT to investigate the circulatory map of the brain and the foot, and to investigate the metabolic process of the cerebrum, the heart, the liver, the thyroid and other organs, and especially to study diseases of the nervous system of the brain, has conspicuous merits.

In the past ten years, the development and use of PECT has been given the greatest possible emphasis by physicists and medical scientists. Thousands have devoted their efforts to research and development in the field. The Berkeley (U.S.A.) Laboratory [2], the European Center for Nuclear Research (CERN) [3], and England's Rutherford Laboratory [4] have developed individually different forms of multiwire positron computerized tomography for nuclear medical research [5]. In addition, first and second generation multiwire proportional chamber (MWPC) PECT is directly used in the field of solid body investigation in physics to measure Fermi surfaces as well as to determine the momentum, distribution and concentration of electrons in metals and alloys [6]. We began to develop MWPC PECT in 1983 and after three years' effort have achieved highly satisfactory results.

This article describes in detail a MWPC positron camera system. It includes a high-density multiwire chamber, readout electronics, computer on-line data gathering, and an image reconstruction process. Using a liquid ^{22}Na positron source to perform simulated static radiography, we achieved three-dimensional tomography with a clear image and stable system operation.

2. Detectors

The two-dimensional readout high-density MWPC is the core of the positron camera. It is composed of a multiwire chamber and a multilayer lead-sheet gamma-ray transforming body [7]. The multiwire chamber has three wire surfaces: the central surface is the anode, and the two cathode surfaces are positioned on both sides of the anode. Reactive signals on the wires of the cathode are used to record incident particles' X and Y coordinates.

Because MWPC is a gas detector operating under atmospheric pressure, it requires an effective detection capacity equivalent to a 511 keV photon; it is necessary first to transform the photons into electrons. Based on this consideration, a gamma-ray transforming body with an effective surface area of 20 cm x 20 cm and a thickness of 6 mm was designed. In order to facilitate the entry of photons/electrons produced in different lead layers in the

transforming body into the sensitive area of the multiwire chamber, it is necessary to add a drift electric field to the transforming body.

An automatic air-mixing system supplies the working gas. The gas is able to move evenly and without obstruction through the transforming body and sensitive area of the MWPC. In order to prevent interference from the external environment, the detector has an effective electronic screen.

There are many methods of reading out the cathode signal of the MWPC; in order to cut down the number of amplifiers and reduce the demands on the quality of the front-rank amplifier, we have chosen the cathode wire coding readout method [8]. Each cathode surface only needs a 28-route amplifier to realize the goal of reading out 192 signal paths.

The major technical specifications for the detector are as follows:

Sensitive area:	20 x 20 cm ²
Working gas:	80% Ar + 20% CO ₂
Anode high voltage:	2.5 kV
Gamma-ray transforming body drift voltage:	-1.0 kV
Readout style:	Reactive pulse cluster center
Spatial resolution:	1 mm
Detection efficiency for 511 keV photon:	5.6%

3. Electronic Readout System

The schematic MWPC positron camera system is shown in Fig. 1. The MWPC's 100 anode wires are joined together and linked with a voltage amplifier [9]. When the anode signal has been amplified, it passes through a constant comparison time-setting filter device (CFD) and reaches a fast coincidence circuit; the coincidence output signal passes out through an exit, giving all coincidence registers a signal to open. The 192 signal wires of each cathode surface are organized into four groups of 24 pairs, and each group and pair is individually coupled with an electric charge sensitive front-rank amplifier.

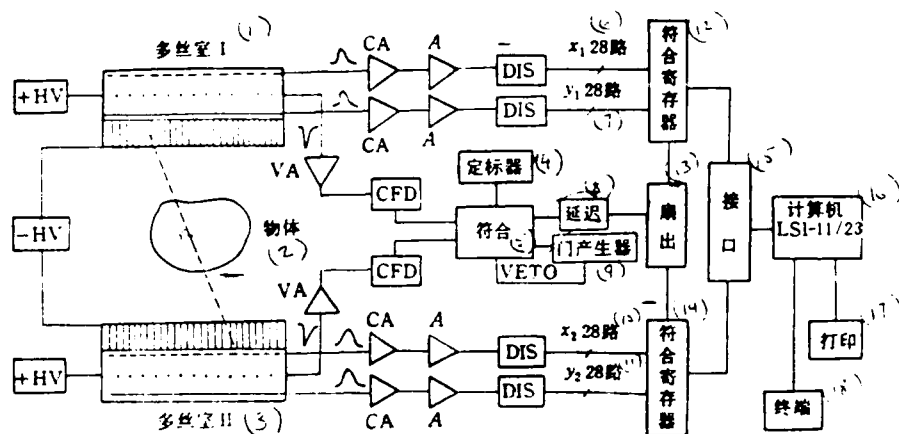


Fig. 1. Schematic for MWPC positron camera system.

Key: (1) MWPC I; (2) object; (3) MWPC II; (4) marker; (5) coincidence; (6) x_1 28 routes; (7) y_1 28 routes; (8) delay; (9) gate producer; (10) x_2 28 routes; (11) y_2 28 routes; (12) coincidence register; (13) exit; (14) coincidence register; (15) connector; (16) LSI-11/23 computer; (17) printer; (18) terminal.

Using an electric charge sensitive amplifier, it is possible to eliminate efficiently the undesirable influence caused by each group/pair's output terminal stray capacitance; at the same time it raises the sensitivity for picking up signals.

The front rank amplifier's output signals are sent through the main amplifier and screening mechanism to a Lecroy 4448 coincidence register. When the gamma rays emitted as a pair by the annihilation of a positron and an electron are detected individually by the detectors, each cathode surface has a group of response pulse outputs which, with the anode trigger signal, implement coincidence registration; and further, passing through a 2912 Uni-Q communication line switching device and a CAMAC 3912 controller, read out the coincidence register's data on the internal storage of the LSI-11/23 computer. The coincidence register is a single-width CAMAC insert having a 16 x 3 register path. Recording the signals of the MWPC's four cathodes are a total of three 4448 registers occupying three positions in the CAMAC controller.

The computer uses the single-user RT-11 operating system, which has a rapid real-time response capacity. The entire on-line transport program uses the dependent program adjusted use method, the user compiling the main program in accordance with actual demand. The computer, on the basis of the evaluation/selection criteria and the reactive pulse cluster center method readout principle, seeks out each cathode pulse cluster's center, and establishes the spatial coordinates (x_1, y_1) , (x_2, y_2) of an authentic photon pair instance.

4. Computerized Image Reconstruction

For image reconstruction, we selected the reprojection wave filter method. If we take the coordinates (x_1, y_1) , (x_2, y_2) of the two gamma rays as measured by the detector, join them with a straight line, and relate the line to the tomographic plane of the object under observation, the line will necessarily pass through the annihilation point of $e^+ e^-$, called the focal point. All instances together comprise a set of focal points, which constitute the focal plane, and this is the above-mentioned tomographic plane's reprojected image. Obviously, the reprojected image, in addition to the actual image formed by the annihilation points on the plane under consideration, also contains background produced on the tomographic plane by cases of annihilation on other planes. The process of using mathematics to eliminate the background is called the wave filter process; the image after undergoing wave filtering reflects the distribution of atomic particles on the tomographic plane [10]. The main steps in the processing of the data are as follows:

- 1) Using the large quantity of measured data, establish the reprojection density distribution function for each tomographic plane; establish the reprojection matrix's Fourier transformation.
- 2) In the transformation matrix each frequency's amplitude is multiplied by the value of the corresponding point response function, to implement the wave filter process.
- 3) An inverse Fourier transformation is implemented on the filtered matrix to return to actual space.

4) The image is smoothed and output.

Under the conditions of our experimentation the investigated bodies were placed between two parallel detectors. Reprojection was a process of projecting the two-dimensional data provided by the MWPC's in three-dimensional space. The mathematical description for realizing the reprojected image wave filter is the Fredholm formula:

$$f_M(x, y, z) = \iiint_{-\infty}^{\infty} f(x', y', z') \cdot h(x, y, z; x', y', z') dx' dy' dz' \quad (1)$$

Here, $f_M(x, y, z)$ represents the reprojected image, that is the experimentally measured radioactivity distribution; $f(x', y', z')$ represents the actual three-dimensional image, that is, the radioactivity distribution that requires solution; $h(x, y, z; x', y', z')$ is the Green function for the imaging system, also called the point response function.

The point response function $h(x, y, z; x', y', z')$ ordinarily is not a spatial constant. If a sufficient number of limits are added, for example limitations to the size of the reconstructed area, it causes the camera to set the somewhat random reception angles in the reconstruction area approximately equal; large angle instances disappear, so that edge effect is lost, and so on. Thus the point response coefficient becomes a spacial constant, which is only the function of $(x - x')$, $(y - y')$, $(z - z')$, and has no relation with the value of any of the points $(x, y, z; x', y', z')$. Hereupon the integral equation (1) becomes the three-dimensional bounded curved volume integral:

$$\begin{aligned} f_M(x, y, z) &= \int_0^{x'} \int_0^{y'} \int_0^{z'} f(x', y', z') \cdot h(x - x', y - y', z - z') dx' dy' dz' \\ &= f_R(x, y, z) \cdot h(x, y, z). \end{aligned} \quad (2)$$

Using the curved volume theorem, formula (2) becomes the product of the frequency range:

$$F_M(K_x, K_y, K_z) = F_R(K_x, K_y, K_z) \cdot H(K_x, K_y, K_z) \quad (3)$$

Here, F_M , F_R , and H are the Fourier transformations of $f_M(x, y, z)$, $f_R(x, y, z)$, and $h(x, y, z)$, respectively.

Formula (3) can be manipulated to produce

$$F_R(K_x, K_y, K_z) = \frac{F_M(K_x, K_y, K_z)}{H(K_x, K_y, K_z)}$$

Using the inverse Fourier transformation, we obtain the desired radioactive nuclide distribution:

$$f_R(x, y, z) = \iiint_{-\infty}^{\infty} F_R(K_x, K_y, K_z) \cdot e^{i(xK_x + yK_y + zK_z)} dK_x dK_y dK_z \quad (4)$$

For the two fixed, limited angle reception MWPC position cameras used in our work, the point response function is:

$$h(x, y, z) = \frac{\cos \theta}{2\pi r^2} = \frac{z}{2\pi(x^2 + y^2 + z^2)^{3/2}} \quad (5)$$

θ is the angle of incidence of the line of annihilation with z axis, $\cos \theta$ is the ruling factor. The point response function is as shown in Fig. 2.

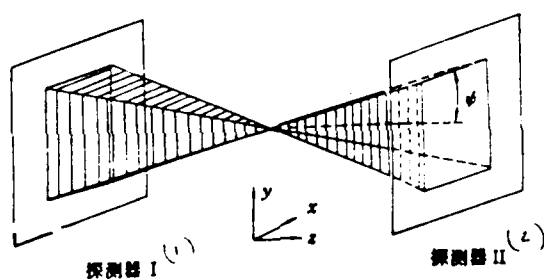


Fig. 2. Point response function. Key: (1) detector I; (2) detector II.

Because the camera has a limited angle of reception, the frequency space point response function $H(K_x, K_y, K_z)$ has a frequency cone equal to zero; within this cone the frequency cannot be measured. The reason lies in the fact that the camera loses the pair of gamma rays produced by the annihilation of positrons outside the angle of reception. The reverse wave filter $G(K_x, K_y, K_z)$ is defined in the broad sense as the opposite of the wave filter $H(K_x, K_y, K_z)$:

$$G(K_x, K_y, K_z) = \begin{cases} H^{-1}(K_x, K_y, K_z) & H \neq 0 \\ 0 & H = 0 \end{cases} \quad (6)$$

Merging (6) into formula (3) we obtain:

$$F_R(K_x, K_y, K_z) = F_M(K_x, K_y, K_z) \cdot G(K_x, K_y, K_z) \quad (7)$$

On the reverse wave filter $G(K_x, K_y, K_z)$, multiplied by the window function $W(K_x, K_y, K_z)$, it is possible effectively to control the effect of the wave filter magnifying the noise within the above-mentioned frequency range, and thereby to improve the quality of the image.

In the process of reconstructing the image, the reverse wave filter with a window function is shown as:

$$G_W(K_x, K_y, K_z) = G(K_x, K_y, K_z) \cdot W(K_x, K_y, K_z) \quad (8)$$

So formula (7) becomes:

$$F_R(K_x, K_y, K_z) = F_M(K_x, K_y, K_z) \cdot G_W(K_x, K_y, K_z) \quad (9)$$

In this manner it is possible to go through an inverse Fourier transformation, obtaining a post-reconstruction radioactive nuclide distribution:

$$f_R(x, y, z) = \iiint_{-\infty}^{\infty} F_R(K_x, K_y, K_z) \cdot e^{2\pi j(xK_x + yK_y + zK_z)} dK_x dK_y dK_z \quad (10)$$

The image reconstructed by the computer is output clearly in shades of gray.

In order to study results of image reconstruction and the influence of various parameters on image quality, we have set up a computer simulated mathematical pattern similar in shape to a human cranium. It consists of the skull, the right and left ventricles, cavities affected by disease, and swollen lumps. Each part is provided with different density distributions of "radioactive nuclides." Using a computer we undertook a random sampling on the model and performed reprojection and image reconstruction processing. A total of 10^6 "instances" was calculated. Figure 3 shows the eighth and ninth section images, including the original image, the reprojection, and the reconstructed image. The results are satisfactory.

$Np=8$

$Np=9$

(a)

(b)

(c)

Fig. 3. Processing of computer simulated image. (a) original; (b) reprojection; (c) reconstructed image.

5. Experimental Results

The MWPC positron camera system is shown in a photograph in Fig. 4. It

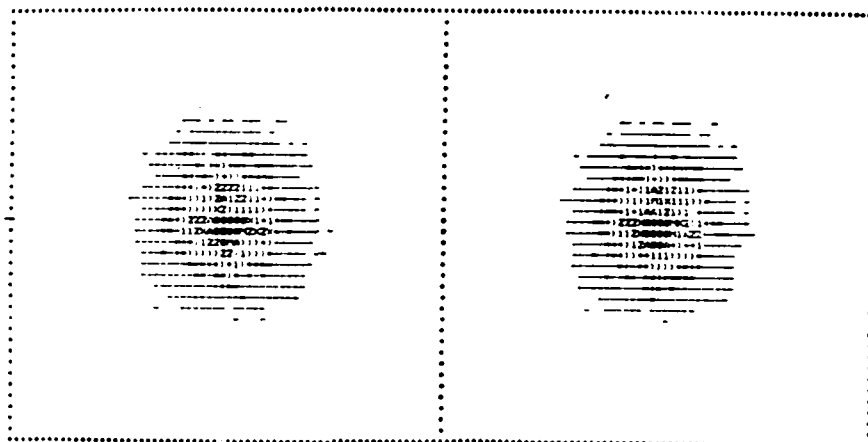


Fig. 4. Multiwire proportional chamber positron camera system.

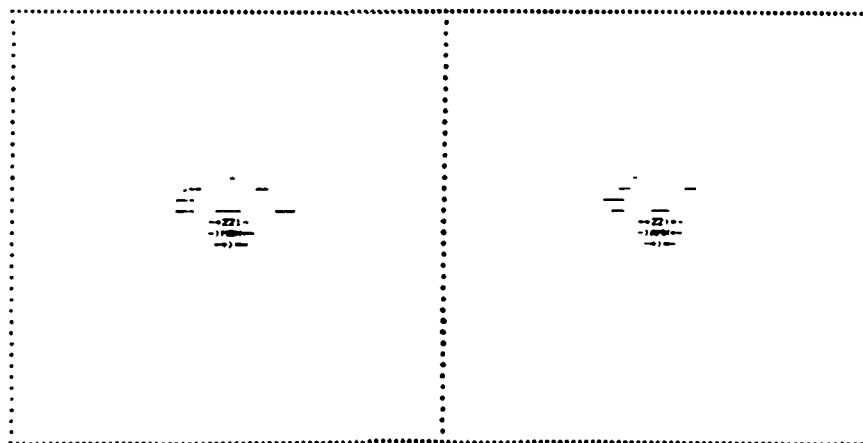
includes the detectors, high voltage electric supply, gas system, NIM and CAMAC electronics with an LSI-11/23 computer having 256 KB of memory and a 40 MB hard disk, a terminal and a printer. The two-high density MWPC's are set up parallel to each other at a distance of 24 cm. The object to be imaged is an iron-sheet cylinder 10 cm in diameter and 15 cm high. In the cylinder is a columnar fluid source of positrons, ^{22}Na , with a strength of 200 microcuries, enclosed in a glass bottle around which was wrapped a sheet of thin lead. This kind of containment had no great effect on the penetration of the 511 keV photon produced by the e^+e^- annihilation.

The dimensions of the imaging space were established as 64 x 64 x 16, the computer on line collected 3×10^4 instances. With data processing and visual output, 16 reprojections and reconstructed images were produced; Figure 5 shows the results. Because of the limitation on the length of this article, we have selected only cuts 5 and 6 of the object center and cuts 13 and 14 of its extreme end. For comparison, the reprojections and the reconstructions are shown in pairs. The three-dimensional size of the ^{22}Na positron source,

as obtained from the reconstructed image, is within a 3 mm error range in comparison with the size of the actual object.

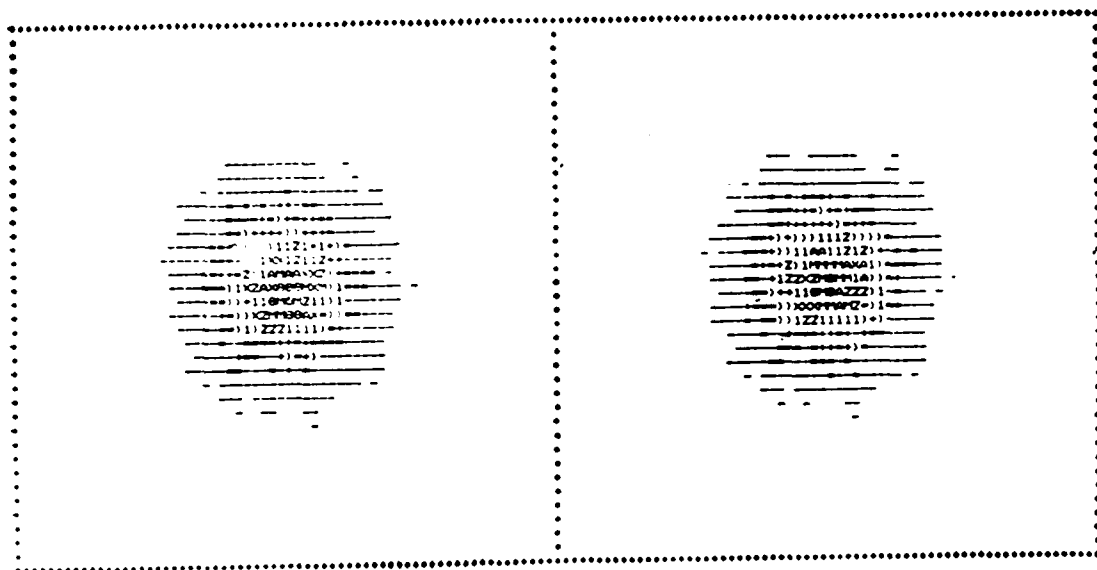


(a)

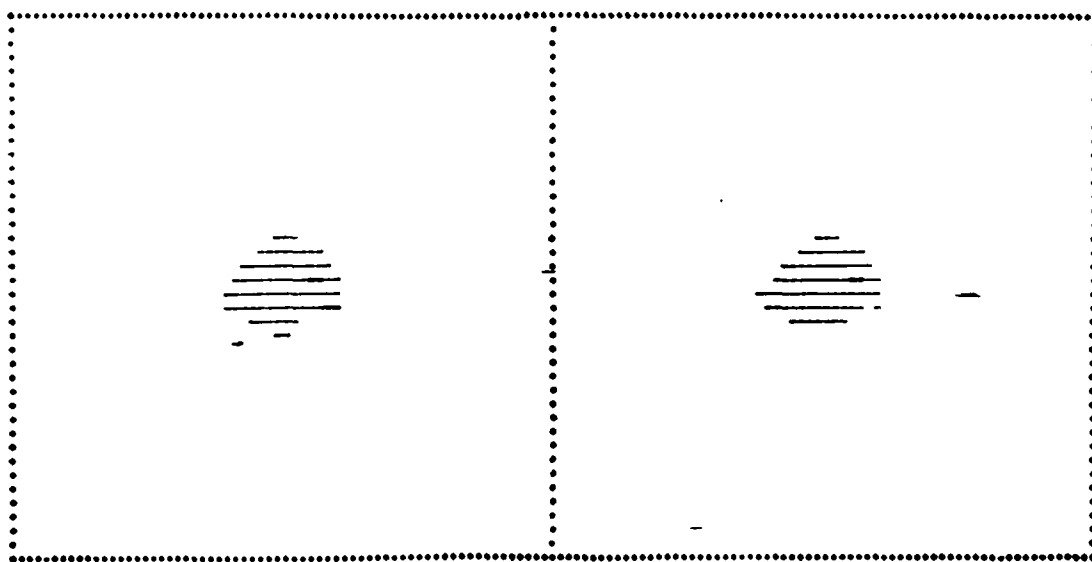


(b)

Fig. 5. Computerized reprojection and reconstructed image for a simulated object. (a) reprojection for cuts 5 and 6; (b) reconstructed image for cuts 5 and 6.



(c)



(d)

Fig. 5. Computerized reprojections and reconstructed images.
(c) reprojection for cuts 13 and 14; (d) reconstructed images for cuts 13 and 14.

Under the conditions of our experiment, the use of the LSI-11/23 to make a reprojection and reconstructed image required about one hour; the use of a VAX-11/780 required only two minutes. To increase the data processing speed of the LSI-11/23, it would be necessary to equip it with a high-speed calculation upgrade, which could reduce the processing time required to a matter of minutes.

Our success in constructing images with simulated objects has laid a good foundation for trials with living objects. With improvements, the system can be used in measuring two gamma angle relations for solid physics investigations.

The authors wish to express their gratitude to Mr. Ye Minghan, our department head, and Mr. Zheng Linsheng for their concern and support of our work. Among our colleagues, Xie Qi participated in preparing the illustrations; Xie Yigang, Yao Zongyuan, Liu Nianzong, and Li Ziping assisted in parts of the work; the leadership of the No. 2 Physics Laboratory and a group of colleagues provided no small measure of assistance and encouragement. Professors Wang Zhuxiang and Zai Guiliang provided this project with great support. We wish to express our heartfelt thanks to them all.

BIBLIOGRAPHY

1. Brownell, Gordon L., and Thomas F. Budinger, Paul C. Lauterbur, Patrick L. McGeer, Science, 5 February 1982, Vol. 215, No. 4533.
2. Del Guerra, A., V. Perez-Mendez, G. Schwartz, IEEE Trans. Nucl. Sci., NS 30 (1983), 646.
3. Jeavons, A., K. Kull, D. Townsend et al., Nucl Instr. and Meth., 176 (1980), 89.
4. Bateman, J.E., J.F. Connolly et al., Nucl. Instr. and Meth., 176 (1980), 83.
5. Bateman, J.E., J.F. Connolly et al., Nucl. Instr. and Meth., 217 (1983), 77.

6. Bisson, P.E. et al., Helv. Phys. Acta, 55 (1982), 100-121.
7. Wang Dewu et al., Gao Neng Wu Li Yu He Wu Li [High Energy Physics and Nuclear Physics], 11 (1987), 589.
8. Wang Dewu, Li Yunshan et al., He Dian Zi Xue Yu Tan Ce Ji Shu [Nuclear Electronics and Detection Technique], 7 (1978), 151.
9. Li Yunshan et al., "The Readout System of the Three-Dimensional Positron CT," Third nuclear electronics and nuclear detector conference, Huang Shan, October 1986.
10. Townsend, D.W. and P. Zanella, CERN - Data Handling Division, DD/80/9, March 1980.

DISTRIBUTION LIST
DISTRIBUTION DIRECT TO RECIPIENT

<u>ORGANIZATION</u>	<u>MICROFICHE</u>
A205 DMAHTC	1
C509 BALLISTIC RES LAB	1
C510 R&T LABS/AVEADCOM	1
C513 ARRADCOM	1
C535 AVRADCOM/TSARCOM	1
C539 TRASANA	1
C591 ESTC	4
C619 MIA REDSTONE	1
D008 MISC	1
E053 HQ USAF/INET	1
E404 AEDC/DOF	1
E408 AFWL	1
E410 AD/IND	1
E429 SD/IND	1
P005 DOE/ISA/DDI	1
P050 CIA/OCR-ADD/SD	2
AFIT LPE	1
FTD	
CCV	1
MIA/PHS	1
LLYL/CODE 1-589	1
NASA/NST-44	1
NSA/T513/TCL	2
ASD/FTD/TOLA	1
FSL/NIX-5	1

FTD-ID(RS)T-0106-89